Ion selectivity and current saturation in inward-rectifier K^+ channels

Lei Yang,[1] Johan Edvinsson,[1] Henry Sackin,[2] and Lawrence G. Palmer[1]

[1]Department of Physiology and Biophysics, Weill-Cornell Medical College, New York, NY 10065
[2]Department of Physiology, The Chicago Medical College, North Chicago, IL 60064

We investigated the features of the inward-rectifier K channel Kir1.1 (ROMK) that underlie the saturation of currents through these channels as a function of permeant ion concentration. We compared values of maximal currents and apparent K_m for three permeant ions: K^+, Rb^+, and NH_4^+. Compared with K^+ (i_{max} = 4.6 pA and K_m = 10 mM at −100 mV), Rb^+ had a lower permeability, a lower i_{max} (1.8 pA), and a higher K_m (26 mM). For NH_4^+, the permeability was reduced more with smaller changes in i_{max} (3.7 pA) and K_m (16 mM). We assessed the role of a site near the outer mouth of channel in the saturation process. This site could be occupied by either permeant ions or low-affinity blocking ions such as Na^+, Li^+, Mg^{2+}, and Ca^{2+} with similar voltage dependence (apparent valence, 0.15–0.20). It prefers Mg^{2+} over Ca^{2+} and has a monovalent cation selectivity, based on the ability to displace Mg^{2+}, of $K^+ > Li^+ \sim Na^+ > Rb^+ \sim NH_4^+$. Conversely, in the presence of Mg^{2+}, the K_m for K^+ conductance was substantially increased. The ability of Mg^{2+} to block the channels was reduced when four negatively charged amino acids in the extracellular domain of the channel were mutated to neutral residues. The apparent K_m for K^+ conduction was unchanged by these mutations under control conditions but became sensitive to the presence of external negative charges when residual divalent cations were chelated with EDTA. The results suggest that a binding site in the outer mouth of the pore controls current saturation. Permeability is more affected by interactions with other sites within the selectivity filter. Most features of permeation (and block) could be simulated by a five-state kinetic model of ion movement through the channel.

INTRODUCTION

In addition to K^+ itself, inward-rectifier K^+ channels conduct other ions including Rb^+, Tl^+, and NH_4^+. In Kir1.1 (ROMK), Rb^+ behaves similarly to K^+ but has a lower conductance and permeability. NH_4^+ is the only other physiologically important cation besides K^+ that is conducted by these channels. The selectivity properties of NH_4^+ are interesting because the relative permeability P_{NH4}/P_K measured under bi-ionic conditions is 0.1, whereas the relative conductance g_{NH4}/g_K is approximately one (Chepilko et al., 1995; Choe et al., 2000). This suggests that NH_4^+ ions can pass through the channels easily but have weaker binding interactions within the pore. K^+ could then readily displace NH_4^+ from the pore, accounting for the low NH_4^+ permeability under bi-ionic conditions.

Inward-rectifier K channels have a high affinity for K^+ ions as assessed by the concentration dependence of conduction. In both Kir1.1 and Kir2.1, currents saturate at low concentrations, with apparent K_m values on the order of 10 mM (Lu and MacKinnon, 1994a; D'Avanzo et al., 2005). In the present study, we investigated the relationship between Kir1.1 cation affinity and permeability. In general, Kir1.1 had lower affinities for less permeable cations. However, the relationship between conductance, permeability, and K_m is complex and appears to involve interactions with different parts of the channel. Permeability depends on binding affinities within the selectivity filter, whereas K_m is strongly influenced by sites outside the filter.

MATERIALS AND METHODS

Expression of Kir1.1 in *Xenopus laevis* oocytes

Oocytes were harvested from *Xenopus* according to the guidelines of, and with the approval of, the Institutional Animal Care and Use Committee of Weill Cornell Medical College. The animals were anesthetized through immersion in 1 liter of tap water containing 1.9 g L^{-1} tricaine methanesulphonate and HEPES (adjusted to pH 7.4) for 5–10 min. Once the animals were anesthetized, a small incision was made in the abdomen and part of the ovary was removed. The oocytes were then dissociated through incubation in OR2 solution (in mM: 82.5 NaCl, 2.5 KCl, 1 $MgCl_2$, 1 Na_2HPO_4, and 5 HEPES, pH 7.4) supplemented with 2 mg ml^{-1} collagenase type II (Worthington) and 2 mg ml^{-1} hyaluronidase type II (Sigma-Aldrich) for 1 h.

pSport plasmids containing Kir1.1b (ROMK2) were linearized with NotI restriction enzyme, and cRNAs were transcribed with T7 RNA polymerase using mMESSAGE mMACHINE T7 kit (Invitrogen). cRNA pellets were dissolved in nuclease-free water and stored at −70°C before use. The oocytes were injected with 10 ng RNA and incubated overnight in L-15 solution supplemented with HEPES, pH 7.4, 63 mg L^{-1} penicillin, and 145 mg L^{-1}

Correspondence to Lawrence G. Palmer: lgpalm@med.cornell.edu
Abbreviation used in this paper: RCR, rate-constant representation.

The Rockefeller University Press $30.00
J. Gen. Physiol. Vol. 139 No. 2 145–157
www.jgp.org/cgi/doi/10.1085/jgp.201110727

streptomycin at 18°C. All chemicals were from Sigma-Aldrich unless otherwise noted.

Patch clamp

Before use, the vitelline membranes of the oocytes were mechanically removed in a hypertonic solution containing 200 mM sucrose. Patch-clamp pipettes were prepared from hematocrit capillary glass (VWR International) using a vertical puller (David Kopf Instruments). They had resistances of 2–8 MΩ when filled with 110 mM KCl. For measurements in inside-out patches, pipette and bath solutions contained Cl^- salts of K^+, Rb^+, and NH_4^+, as indicated, plus 5 mM HEPES buffered to pH 7.4. In addition, bath solutions contained 0.5 mM EDTA. Currents from cell-attached and excised inside-out patches were recorded with a patch-clamp amplifier (EPC-7; HEKA), digitized with an interface (Digidata 1332A; Axon Instruments). Data were filtered at 1 kHz and analyzed with pCLAMP9 software (Axon Instruments).

Data analysis

Currents were measured from selected recording intervals normally containing a single active channel using all-points histograms. Histograms were fit with double Gaussian functions, and the current amplitude was defined as the distance between the two peaks.

Single-channel currents (i) were analyzed according to the equation:

$$i = i_{max} / \left(1 + K_m / \left[C^+\right]\right), \quad (1)$$

where $[C^+]$ is the concentration of the permeant ion.

The effects of external blocking ions were analyzed according to the equation:

$$i(B) = i(0) / \left(1 + [B] / K_i\right), \quad (2)$$

with

$$K_i(V) = K_i(0) \cdot \exp(z\delta FV/RT), \quad (3)$$

where [B] is the blocker concentration, z is the blocker valence, V is the transmembrane voltage, and δ is the effective valence or fraction of the electric field at the blocking site. $K_i(0)$ and δ were estimated from linear regression analysis of a linearized form of Eq. 2:

$$\ln\left(i(0)/i(B) - 1\right) = \ln\left([B]/K_i(0)\right) - z\delta FV/RT.$$

Kinetic modeling

The kinetic model shown in Fig. 10 was evaluated using Matlab 7.8.0 as described previously (Edvinsson et al., 2011). Rate constants were calculated based on the values set for binding energies, energy barriers, and electrical distances. The values for the fractional electrical distances δ_1, δ_2, and δ_3 were 0.07, 0.113, and 0.233, respectively, as used in previous studies (Kutluay et al., 2005). The model was fitted to the appropriate experimental data using the *lsqcurvefit* function in Matlab.

Online supplemental material

Online supplemental material shows the effects of external Na^+ on K^+ currents in the presence of the divalent cation chelator EDTA (Fig. S1). Figs. S2 and S3 illustrate the sensitivities of the measurable parameters of conductance, apparent K_m, and bi-ionic reversal potentials simulated by these models to changes in the binding energies to the different sites. Table S1 lists the kinetic parameters of the permeation model based on fits to experimental data. Figs. S1–S3 and Table S1 are available at http://www.jgp.org/cgi/content/full/jgp.201110727/DC1.

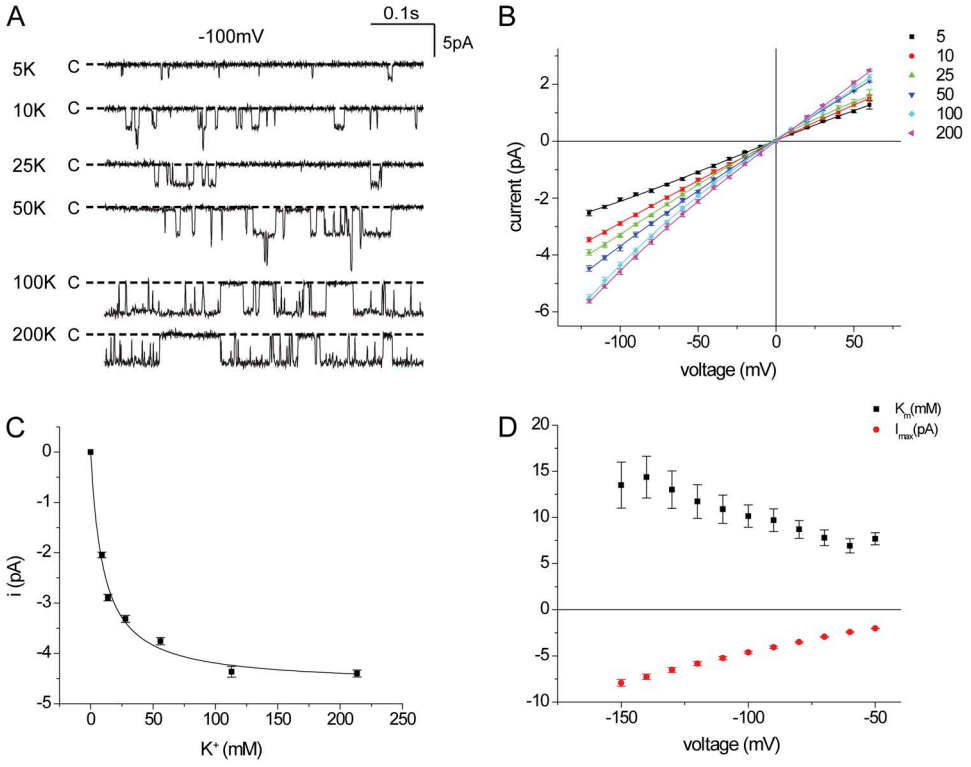

Figure 1. Conduction through Kir1.1 channels in inside-out patches with symmetrical K^+ concentrations. (A) Inward currents with −100 mV across the patch at different $[K^+]$. (B) i-V relationships for different $[K^+]$. Lines through the data points have no theoretical meaning. (C) Single-channel currents at −100 mV as a function of ion concentration. The line represents the best fit of Eq. 1 to the data, with i_{max} = 4.6 ± 0.1 pA and K_m = 10.2 ± 1.2 mM. (D) i_{max} and K_m, measured as in C, as a function of voltage.

RESULTS

Conductance–concentration relationships

We first confirmed the relationship between K^+ concentration and inward currents in Kir1.1 channels. Channels were expressed in *Xenopus* oocytes, and excised inside-out patches were formed with identical K^+ concentrations, ranging from 5 to 200 mM, on both sides of the membrane. K^+ was increased by the addition of KCl to the basic medium without cation substitution. Typical inward current traces for a membrane potential of −100 mV are shown in Fig. 1 A, and the corresponding i-V relationships are plotted in Fig. 1 B. At low K^+ concentrations, the open probability decreased sharply. Decreased open times, together with decreased currents, determined the lower limit of $[K^+]$ at which currents could be resolved. The i-V relationships were approximately linear over the range of −20 to −100 mV at all concentrations. Plotting the current as a function of ion concentration at −100 mV indicated a hyperbolic relationship with a maximal inward current (i_{max}) of −4.6 pA and an apparent K_m of 10.2 mM (Fig. 1 C). The K_m value decreased mildly with depolarization of the membrane voltage, suggesting different voltage dependencies of rates of entering and exiting the channel (Fig. 1 D). Outward currents were less reliably measured as a result of faster kinetics and increased noise levels.

We repeated these experiments using Rb^+ as the conducted ion. Fig. 2 A shows inward currents at −100 mV in inside-out patches with various Rb^+ concentrations from 10 to 200 mM on both sides of the membrane. Fig. 2 B shows i-V relationships for these concentrations. Rb^+ currents were lower than those for K^+, confirming previous findings (Chepilko et al., 1995; Choe et al., 2000). At −100 mV, i_{max} was 1.8 pA, whereas the apparent K_m was 26 mM, higher than that for K^+ (Fig. 2 C). The i-V relationship for Rb^+ was less linear than that for K^+; inward currents increased more rapidly with hyperpolarization. In contrast, the voltage dependence of the apparent K_m for Rb^+ conduction was less than that for K^+ (Fig. 2 D). The lower affinity for conduction correlates with the reduced permeability for this ion relative to K^+, estimated from bi-ionic reversal potentials (Chepilko et al., 1995; Choe et al., 2000).

We also examined the concentration–conductance relationships for NH_4^+. Handling of this ion is unusual in that it has a permeability ratio P_{NH4}/P_K of only ∼0.1, determined from reversal potential measurements, but its conductance is comparable to that of

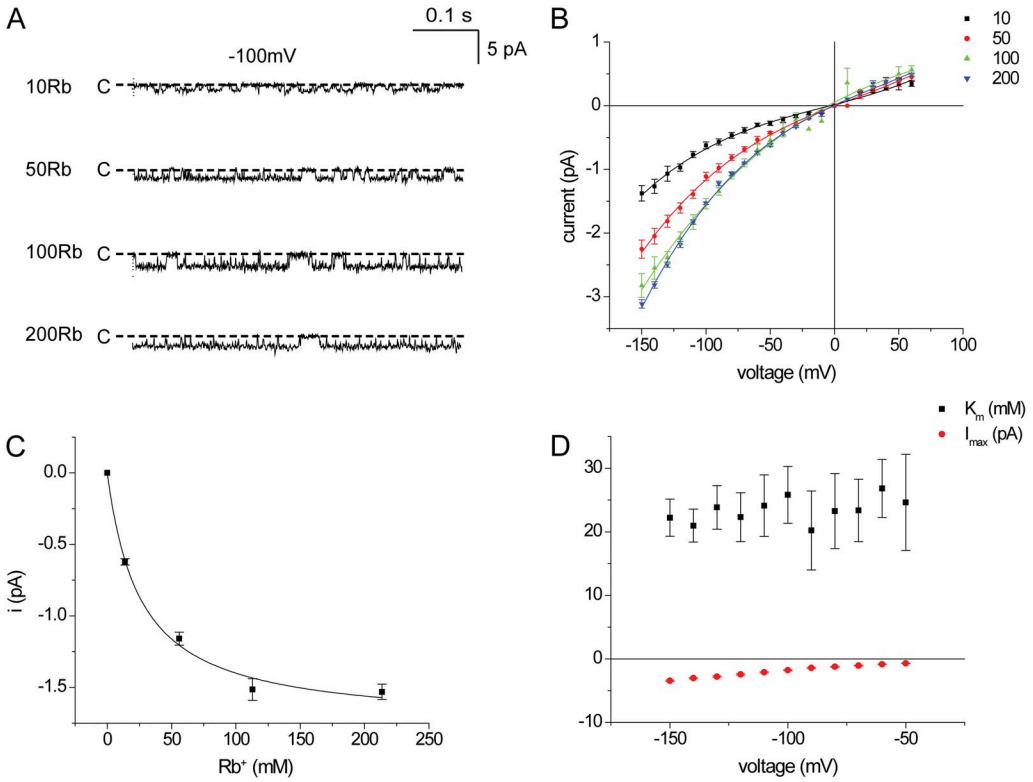

Figure 2. Conduction through Kir1.1 channels in inside-out patches with symmetrical Rb^+ concentrations. (A) Inward currents with −100 mV across the patch at different $[Rb^+]$. (B) i-V relationships for different $[Rb^+]$. Lines through the data points have no theoretical meaning. (C) Single-channel currents at −100 mV as a function of ion concentration. The line represents the best fit of Eq. 1 to the data, with i_{max} = 1.8 ± 0.1 pA and K_m = 26 ± 4 mM. (D) i_{max} and K_m, measured as in C, as a function of voltage.

K^+ (Chepilko et al., 1995; Choe et al., 2000). We hypothesized that the low permeability might be explained if NH_4^+ interacted less strongly (i.e., were bound less tightly) than K^+ as it traversed the channel, predicting a higher apparent K_m for conduction. Current traces for NH_4^+ are shown in Fig. 3 A, and i-V relationships are shown in Fig. 3 B. As found previously (Choe et al., 2000), the channel kinetics change when NH_4^+ is conducted, with much briefer openings and lower open probability. With low NH_4^+ concentrations, the open times were further decreased, limiting the lower end of the usable concentration range to 25 mM. As shown in Fig. 3 C, the maximal inward current for NH_4^+ was 3.7 pA at −100 mV, whereas the apparent K_m value was 16 mM, higher than but not strikingly different from that for K^+. The voltage dependence of K_m was small, at least between −60 and −150 mV (Fig. 3 D). However, outward NH_4^+ currents were virtually independent of NH_4^+ concentration over this range (Fig. 3 B), implying that the K_m for conduction in this direction was well below those for inward currents. However, as with K^+, these currents were more difficult to measure accurately.

To see if the saturation of NH_4^+ currents is affected by the presence of K^+ on the opposite side of the membrane, we investigated inside-out patches in which NH_4^+ was varied only in the pipette (extracellular) solution with constant 110 mM K^+ in the bath. Because the reversal potential changes under these conditions, we analyzed inward NH_4^+ slope conductances, rather than currents, over the concentration range of 50–200 mM (Fig. 4). These conductances (60–80 pS) were larger than those measured under symmetrical conditions for K^+ or NH_4^+. There was little change in conductance over this concentration range, again indicating high-affinity interactions with the channel.

Occupancy of an outer binding site

One possible site of interaction of permeant ions with the channel that could contribute to saturation of currents is the outer mouth of the pore, just external to the selectivity filter. This could contain an obligatory binding site for ions that controls the rate of movement into the channel. Analysis of a multi-ion pore with simplified association–dissociation kinetics showed that the presence of such a site could lead to Michaelis–Menten-type kinetics of permeation (Nelson, 2011). Similar results are presented below for a more complex kinetic scheme.

Because such a site might not be as strongly ion selective as those of the filter itself, we examined whether the smaller alkali metal cations Na^+ and Li^+ could reduce K^+ conductance through the channel by competing for occupancy. Fig. 5 (A and B) shows traces and i-V relationships in inside-out patches with 110 mM K^+ on the cytoplasmic side and either 11 mM K^+ alone or 11 mM K^+ plus 99 mM Na^+ on the extracellular side of the membrane. The effects of Na^+ were modest but clear. Outward currents were virtually unaffected, whereas inward currents were reduced by 50% or more.

We analyzed these results using a simple Woodhull-type model (see Eqs. 2 and 3 in Materials and methods)

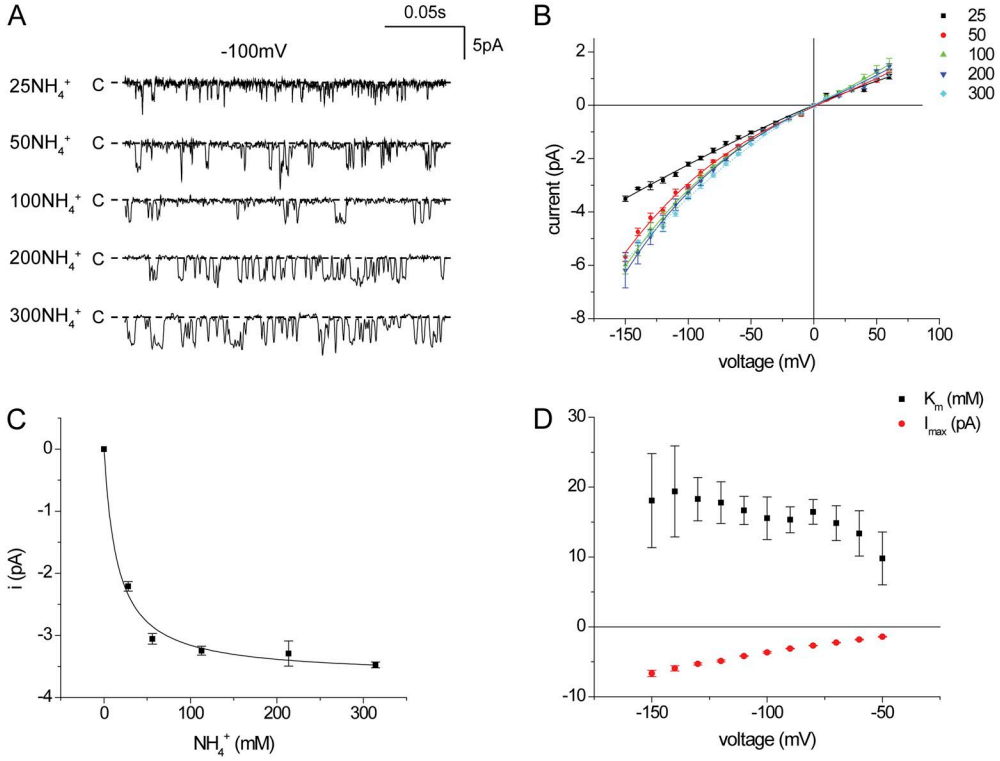

Figure 3. Conduction through Kir1.1 channels in inside-out patches with symmetrical NH_4^+ concentrations. (A) Inward currents with −100 mV across the patch at different $[NH_4^+]$. (B) i-V relationships for different $[NH_4^+]$. Lines through the data points have no theoretical meaning. (C) Single-channel currents at −100 mV as a function of ion concentration. The line represents the best fit of Eq. 1 to the data, with i_{max} = 3.7 ± 0.1 pA and K_m = 16 ± 3 mM. (D) i_{max} and K_m, measured as in C, as a function of voltage.

that assumes a blocking site at a fixed point within the transmembrane electric field. The results of this analysis are shown in Fig. 5 D, in which the equation for fractional block is linearized with respect to voltage. The apparent $K_I(0)$ obtained by extrapolating the linear regression line to V = 0 was 272 mM, whereas the slope of the line gave an effective valence of the blocking reaction of 0.15. That is, the voltage dependence of block could be explained by Na^+ blocking at a site that senses 15% of the transmembrane electric field. In this interpretation, the effects of Na^+ appear as a reduction in single-channel current rather than a decreased open time because the blocking kinetics are too fast to resolve.

Very similar results were obtained with Li^+ (Fig. 5, B and C). In this case, the estimated $K_I(0)$ was 203 mM and the effective valence was 0.17. The voltage dependence of the reduction suggests that Na^+ and Li^+ also bind weakly but specifically within the permeation pathway.

Divalent cations interact with an outer binding/blocking site

We next asked whether divalent cations could block the channel in a similar manner. Fig. 6 (A and B) shows traces and i-V relationships with 11 mM K^+ (and 99 mM Na^+) in the pipette in the absence of divalents and in the presence of Ca^{2+} or Mg^{2+}. Both Ca^{2+} and Mg^{2+} produced a voltage-dependent decrease in current, but the Mg^{2+}-dependent block was stronger. Fig. 6 C shows the analysis of the voltage dependence; the $K_i(0)$ for Ca^{2+} was about threefold higher than that for Mg^{2+}, whereas the effective valences were similar. These values of 0.17 to 0.18 are close to those measured for Na^+ and Li^+, despite the fact that these blockers carry twice the positive charge. The voltage dependence of the block as well as the selectivity between these two divalent cations for block provides further evidence for a specific interaction with the pore.

We extended these results by examining block by 3 mM Mg^{2+} at different extracellular K^+ concentrations. The effects of Mg^{2+} are similar in each case, but the magnitude of current reduction increases as K^+ decreases. This is shown quantitatively in Fig. 7 A. The $K_i(0)$ values, interpolated with 11 mM K^+ and extrapolated with 55 and 110 mM, increase with K^+ concentration, whereas the slopes of the plots are similar. The Ki(0) values are plotted as a function of K^+ in Fig. 7 B. The approximately linear relationship is consistent with a competitive interaction between K^+ and Mg^{2+}, with an estimated K_i for Mg^{2+} in the absence of K^+ of 2.5 mM and a dissociation constant of 15 mM for K^+ binding to the Mg^{2+}-blocking site. This is similar to the apparent K_m for conduction (11 mM) in the absence of blocking ions,

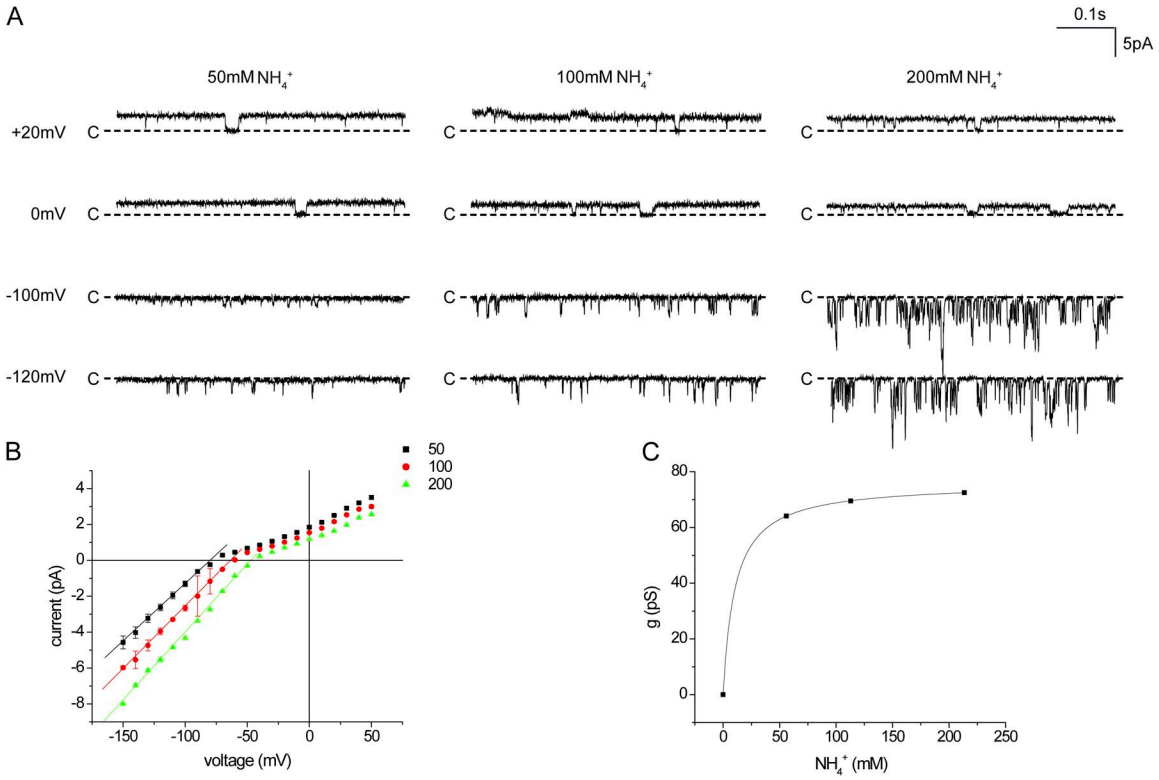

Figure 4. Conduction through Kir1.1 channels in inside-out patches with 110 mM K^+ in the bath solution and different $[NH_4^+]$ in the pipette. (A) Currents at different voltages and $[NH_4^+]$. (B) i-V relationships for different $[NH_4^+]$. Lines through the data points have no theoretical meaning. (C) Inward single-channel conductance measured as the slope of the i-V plots between −60 and −150 mV. The line represents the best fit of Eq. 1 to the data, with g_{max} = 76 ± 1 pS and K_m = 10.4 ± 0.1 mM.

suggesting that this site may well contribute to conductance saturation.

We assessed the selectivity of this site by comparing the ability of different monovalent cations to relieve Mg^{2+} block. This was assessed as the ratio of currents at −100 mV with and without 3 mM Mg^{2+} and is plotted in Fig. 7 C. For Rb^+ and NH_4^+, external K^+ was completely replaced by these ions. For Na^+ and Li^+, 99 mM of the test ion was added to a solution containing 11 mM K^+. These results indicate that the site is somewhat selective for K^+; the other ions tested had similar abilities to displace Mg^{2+}, with Na^+ and Li^+ being slightly more effective than Rb^+ or NH_4^+.

If this outer binding site determines saturation of currents, competition between K^+ and Mg^{2+} in the outer part of the permeation path predicts that Mg^{2+} should shift the apparent affinity of the channel for K^+. To test this, we repeated the measurements of concentration–conductance relationships for K^+ in the presence of 3 mM Mg^{2+} (Fig. 7 D). Under these conditions, the apparent K^+ affinity decreased markedly, with apparent K_m values increasing from 11 to 96 mM. This is consistent with the idea that saturation of K^+ conductance involves K^+ occupancy of the outer binding/blocking site, at least when Mg^{2+} is present in the external solution.

Role of fixed negative charges in saturation and block

Affinities for ions at the outer mouth of the pore should be affected by the presence of fixed negative charges in the extracellular domain of the channel protein (D'Avanzo et al., 2005; Chang et al., 2010). To test this, we mutated several aspartate and glutamate residues in the outer mouth of the pore (E92, D97, E104, and E132) to eliminate their negative charges. The largest effect was observed with alterations at the E104 position; this side chain is situated just above the outer aspect of the selectivity filter (Fig. 8 A). The E104S mutant significantly reduced the efficacy of Mg^{2+} block without changing the voltage dependence (Fig. 8 B). We also studied a quadruple mutant in which all four negatively charged amino acids in the extracellular domain were neutralized. Again, the affinity for Mg^{2+} was decreased modestly but significantly, whereas the voltage dependence remained constant (Fig. 8 C).

The elimination of negative charges did not have much effect on the apparent affinity for K^+ (Fig. 8 D). This result

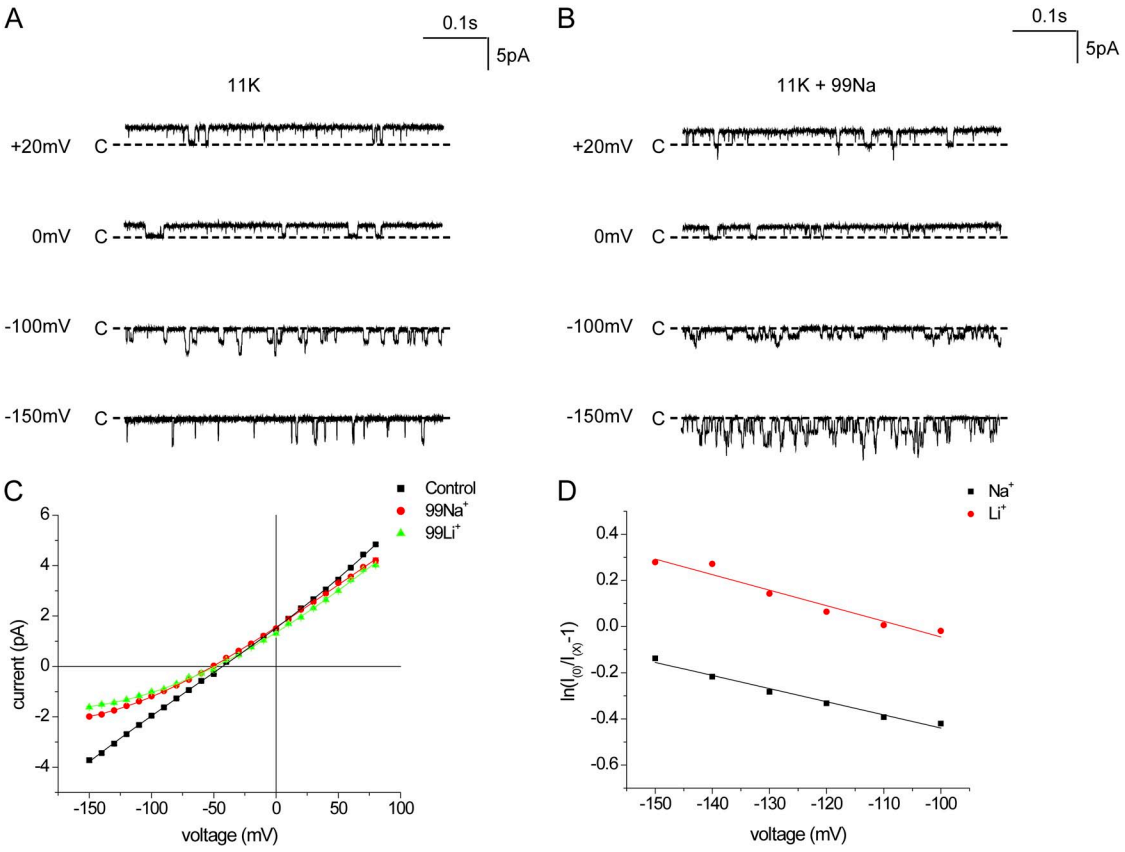

Figure 5. External Na^+ and Li^+ block K^+ currents through Kir1.1 channels. (A) Currents at different voltages in the presence of 11 mM K^+ in the pipette solution and 110 mM K^+ in the bath solution. (B) Currents under the same conditions as in A but with 99 mM Na^+ in the pipette solution. (C) i-V relationships in the absence of blockers and in the presence of 99 mM Na^+ or Li^+ in the external solution. (D) Analysis of block by external Na^+ and Li^+ according to Eqs. 2 and 3. The lines represent best fits to the data, with K_{iNa} = 272 mM and $z\delta_{Na}$ = 0.15, and K_{iLi} = 203 mM and $z\delta_{Li}$ = 0.17.

did not support the idea that the K_m reflects binding to the outer mouth. However, we considered the possibility that the charges might be screened, particularly by trace metal cations in the solutions. Indeed, inclusion of 0.5 mM EDTA to chelate divalent cations significantly decreased the apparent K_m to values too low to measure accurately (Fig. 8 D). The chelator did not change the K_m in mutant channels lacking the negative charges in the outer mouth, consistent with the idea that the charges do affect affinity but are partially screened by residual divalent cations under most conditions. EDTA also modestly increased the block of the channels by extracellular Na^+ (Fig. S1).

In some Kir channels, fixed negative charges in the transmembrane cavity enhance the affinity for block by Mg^{2+} and polyamines (Lu and MacKinnon, 1994b; Taglialatela et al., 1995; Yang et al., 1995). To see if such charges on the other side of the selectivity filter could also influence current saturation, we used the Kir1.1b mutant N152D, in which an aspartate is inserted in the second membrane-spanning segment at the position corresponding to D172 of IRK1. Indeed, there was a significant decrease in the apparent K_m for K^+ conductance, from 10.2 ± 1.2 (Fig. 1) to 4.7 ± 1.4 mM (Fig. 9). The effect is in the same direction as, but much smaller than, the increase in affinity for block by Mg^{2+} or spermine block from the cytoplasmic side of the pore (Lu and MacKinnon, 1994b; Taglialatela et al., 1995; Yang et al., 1995).

Kinetic modeling

To examine if the saturation properties of the Kir1.1 channel could be accounted for with standard models of K^+ channel permeation, we used a five-state scheme used previously to describe KcsA channels (Kutluay et al., 2005) and Kir4.1 channels (Edvinsson et al., 2011). The model can be formulated in terms of rate constants between the states of the channel as described in Fig. 10 A. This scheme is based on known properties of the selectivity filter of K^+ channels. Because Kir1.1 and other inward rectifiers contain a cytoplasmic domain that may provide an additional resistance to ion flow (Choe et al., 2000), the step between the cavity and the internal solution would include movement through this part of the pore.

The model could fit data for i-V relationships with symmetric K^+ or NH_4^+ concentrations, but many different parameter sets gave equally good fits. We then

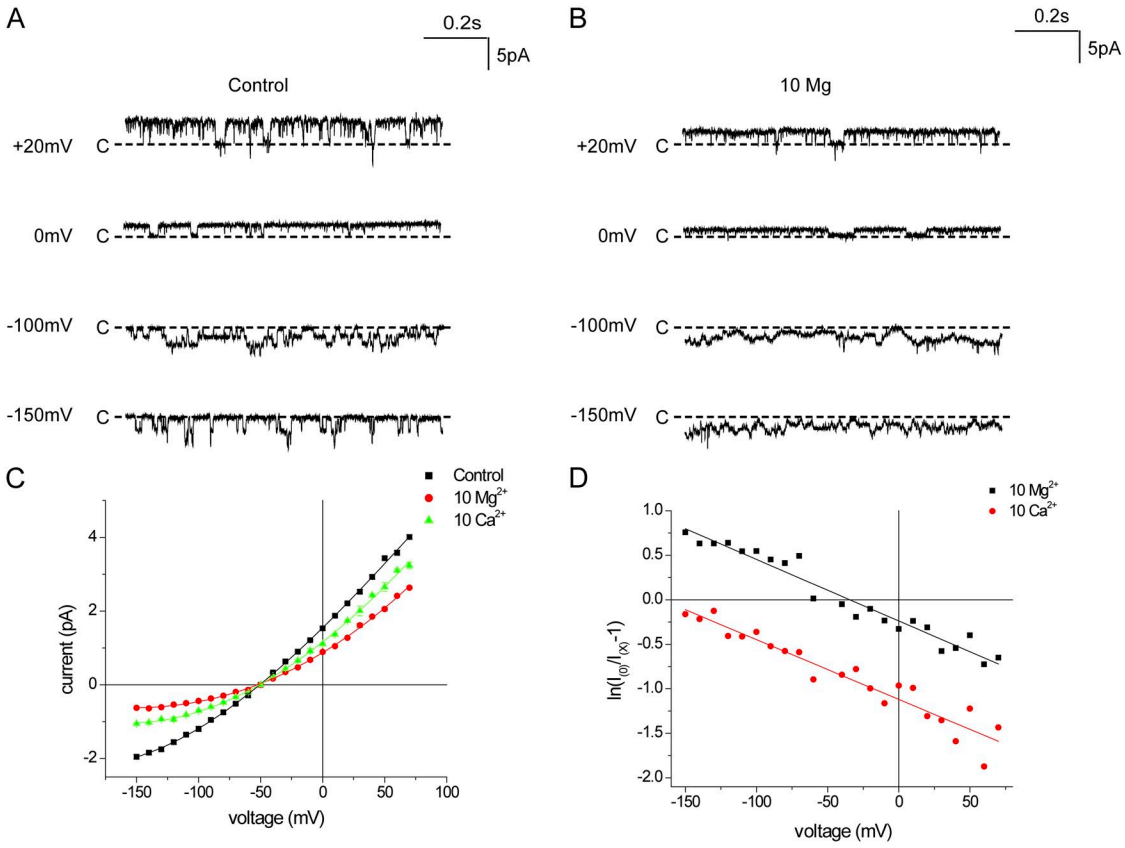

Figure 6. External Mg^{2+} and Ca^{2+} block K^+ currents through Kir1.1 channels. (A) Currents at different voltages in the presence of 11 mM K^+ plus 99 mM Na^+ in the pipette solution and 110 mM K^+ in the bath solution. (B) Currents under the same conditions as in A but with 10 mM Mg^{2+} in the pipette solution. (C) i-V relationships in the absence of divalents and in the presence of 10 mM Mg^{2+} or 10 mM Ca^{2+} in the external solution. (D) Analysis of block by external Mg^{2+} and Ca^{2+} according to Eqs. 2 and 3. The lines represent best fits to the data, with K_{iMg} = 13 mM and $z\delta_{Mg}$ = 0.18, and K_{Ca} = 31 mM and $z\delta_{Ca}$ = 0.17.

attempted to simultaneously fit data from symmetrical K^+, symmetrical NH_4^+, and bi-ionic K^+ versus NH_4^+ conditions. We assumed the same kinetic scheme with the same number of sites and barriers with the same placement within the electric field for the two ions. Only the rates of transitions among the states were allowed to vary. A parameter set that gave satisfactory results is illustrated in Fig. 10 (B–E). The pseudo-energy profiles for NH_4^+ and K^+ along the pore for this set are shown in Fig. 10 F. These values are plotted as "rate-constant representation" (RCR) units (Andersen, 1999), arbitrarily assuming a frequency factor for the Eyring transition-state reaction rates of 6×10^{10} s^{-1}. The actual rates used are given in Table S1.

These parameters were able to reproduce the basic properties of K^+ conduction as well as several of the remarkable features of the NH_4^+ data, including the near independence of outward currents on ion concentration, the high conductance to NH_4^+ despite the low bi-ionic permeability, and the increased inward NH_4^+ conductance with K^+ on the inside of the membrane. One prediction of the model that is different from the experimental observations is the slight decline in currents at high NH_4^+ concentrations. The main features of the parameter set for NH_4^+ are decreased depths of energy wells for NH_4^+ compared with K^+, particularly at sites S1 and S2. Although other parameter sets could also successfully fit the data, all of them involved similar changes at these sites. Thus, this simplified model of ion permeation can largely account for movements of K^+ and NH_4^+ through the channel.

We also performed a sensitivity analysis to examine the influence of model parameters on the predicted observables of apparent K_m, conductance, and reversal potentials. When the binding sites were altered by simultaneously changing the energies of the well and adjacent barriers, the apparent K_m values were most sensitive to increases in S0; increases of 1.3 RCR increased K_m by nearly 10-fold (Fig. S2 A). Changes in S1 had smaller effects, whereas K_m values were almost independent of S2-binding energies. This may reflect the nature of the kinetic scheme, as the model is constrained such that the S1–S4 sites' selectivity filter is occupied by two ions at all times. In contrast, inward conductance through the channel was most sensitive to changes in S1 (Fig. S2 B).

Under bi-ionic conditions, with the parameters for the internal ion fixed (to those estimated for K^+) and those for the external ion varied, reversal potentials were inversely related to the binding energy at each of the sites. When all sites were raised or lowered simultaneously, an increase of 1 RCR produced a reversal potential of −60 mV (Fig. S3 A). These changes also reduced the open-channel conductance by ∼50% (Fig. S3 B).

The decreased energy wells for NH_4^+ account for the decreased P_{NH4}/P_K ratio because under bi-ionic conditions, the sites will be preferentially occupied by K^+.

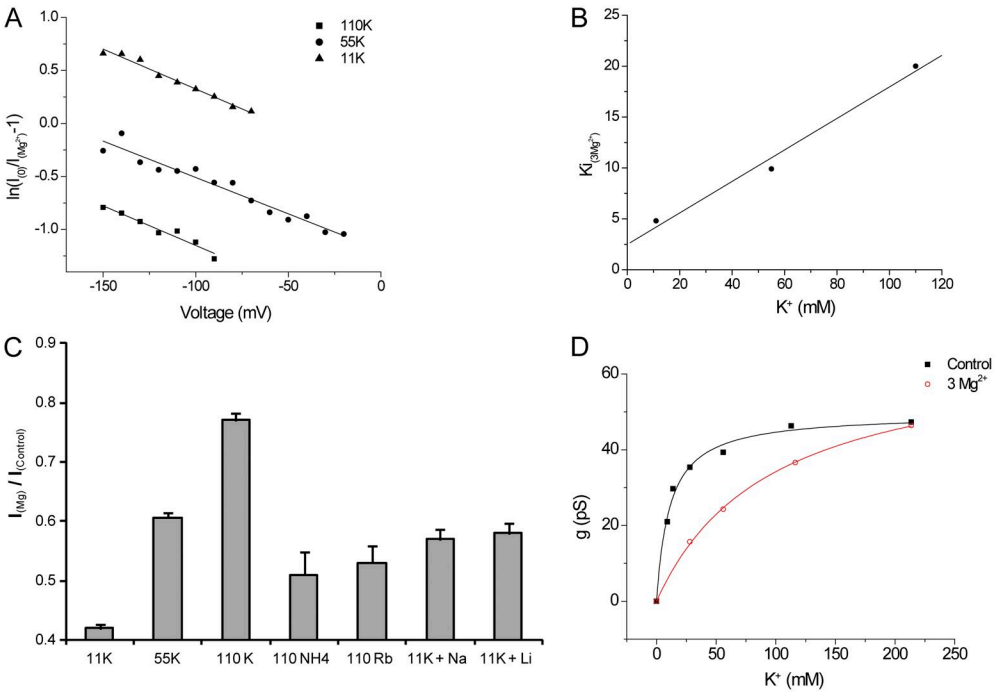

Figure 7. External K^+ competes with Mg^{2+} block of Kir1.1 currents. (A) Analysis of block of K^+ currents by 3 mM Mg^{2+} at three different external [K^+] according to Eqs. 2 and 3. Lines represent $K_{Mg}(0)$ = 4.6 mM and $z\delta_{Mg}$ = 0.19 (11 mM K^+); $K_{Mg}(0)$ = 9.9 mM and $z\delta_{Mg}$ = 0.18 (55 mM K^+); and $K_{Mg}(0)$ = 20 mM and $z\delta_{Mg}$ = 0.19 (110 mM K^+). (B) $K_{Mg}(0)$ plotted versus [K^+]. The straight line represents a linear regression fit of the data. The intercept on the ordinate implies that K_{Mg} = 2.5 mM in the absence of K^+, and the slope provides an estimate of 15 mM for the dissociation constant for K^+ displacement of Mg^{2+}. (C) Ratios of currents at V_m = −100 mV in the presence and absence of 3 mM Mg^{2+} with different ions in the external solution. (D) External Mg^{2+} decreases the apparent affinity for K^+. g is plotted as a function of [K^+] for no added divalents (black) and with 3 mM Mg^{2+} in the external solution (red). Lines represent the best fits to Eq. 1, with g_{max} = 50 ± 1 pS and K_m = 11.0 ± 1.3mM (control), and g_{max} = 67 pS ± 1 and K_m = 96 ± 4 mM (+3 mM Mg^{2+}).

The concomitant high inward NH_4^+ conductance is a distributed property of the various energy barriers and is not so simply accounted for by any one parameter. We have not explored in depth the basis for other properties, such as the higher inward NH_4^+ conductance in the presence of internal K^+ or the low apparent K_m for outward NH_4^+ currents.

DISCUSSION

The main conclusions of this study are: (a) Currents through Kir1.1 channels carried by NH_4^+ saturate with a low apparent K_m only modestly higher than that for K^+, despite a reduced NH_4^+ permeability. (b) Saturation of inward currents partly reflects occupancy of an outer binding site that is selective for K^+ but also accepts other monovalent and divalent cations. (c) The unusual permeation properties of the NH_4^+ ion can be accounted for by conventional kinetic models of ion transport through Kir1.1. These topics are discussed in more detail below.

Saturation of K^+ currents

We found that currents through Kir1.1 channels saturated at low K^+ concentrations, with apparent K_m values of ~10 mM. This is in general agreement with previous results on Kir1.1 (Lu and MacKinnon, 1994a) and Kir2.1 (Lopatin and Nichols, 1996; D'Avanzo et al., 2005; Chang et al., 2010), although the analyses of the concentration dependence varied. At very high K^+ concentrations (>300 mM), conductances through Kir1.1 channels can actually decline from maximal values

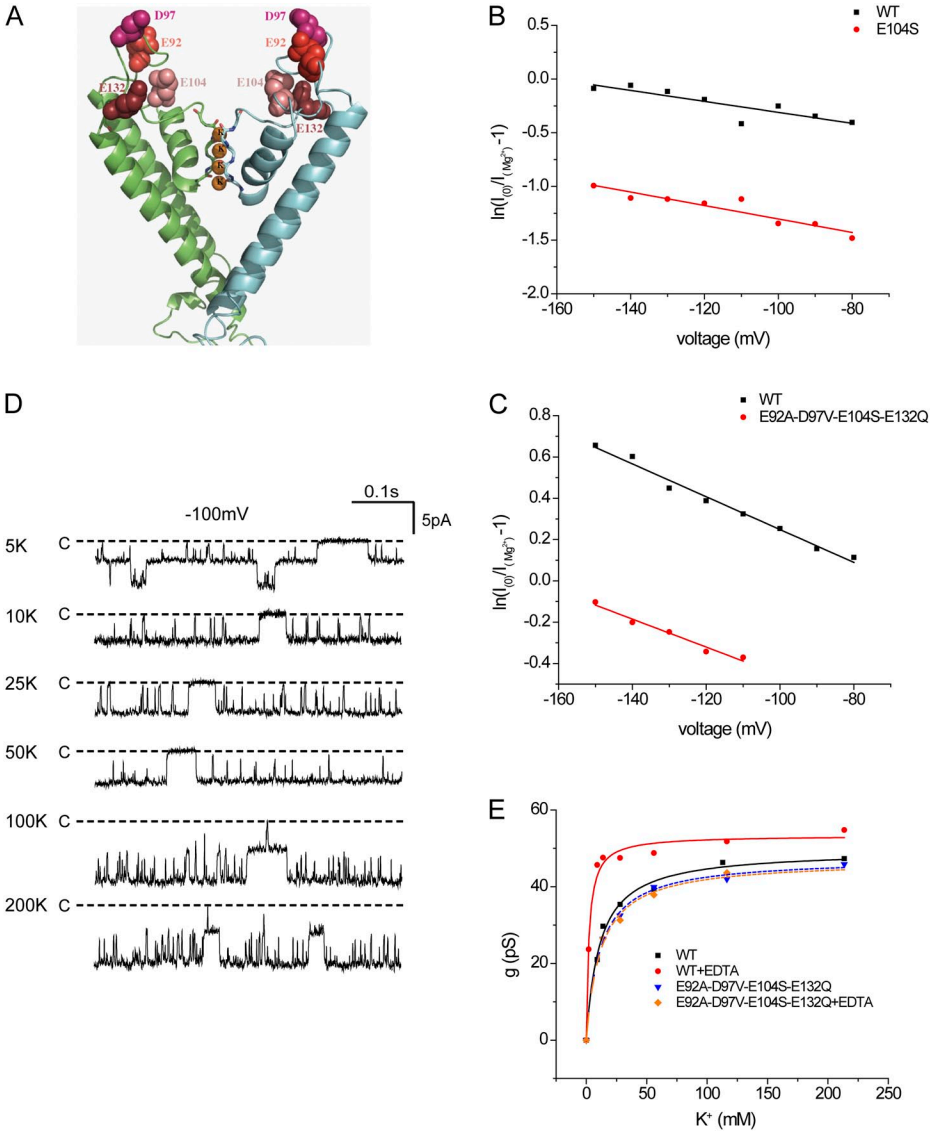

Figure 8. Removal of external fixed negative charges reduces affinity for Mg^{2+} block and K^+ permeation. (A) Homology model of the outer mouth of Kir1.1b showing the positions of four negatively charged amino acid side chains, E92, D97, E104, and E132, relative to the conduction pathway. (B) Analysis of block by 3 mM Mg^{2+} of wild-type (WT) ROMK and the mutant E104S. The internal solution contained 110 mM K^+. The external solution contained 11 mM K^+ plus 99 mM Na^+. Lines represent fits to Eqs. 2 and 3, with $K_{Mg}(0)$ = 3.9 mM and $z\delta_{Mg}$ = 0.16 (WT), and $K_{Mg}(0)$ = 20 mM and $z\delta_{Mg}$ = 0.16 (E104S). (C) Analysis of block by 3 mM Mg^{2+} of WT ROMK and the quadruple mutant E92A/ D97V/ E104S/E132Q. The internal solution contained 110 mM K^+. The external solution contained 11 mM K^+ and no Na^+. Lines represent fits to Eqs. 2 and 3, with $K_{Mg}(0)$ = 5.2 mM and $z\delta_{Mg}$ = 0.20 (WT), and $K_{Mg}(0)$ = 9.3 mM and $z\delta_{Mg}$ = 0.17 (E92A/ D97V/ E104S/E132Q). (D) Current traces for WT Kir1.1b in excised inside-out patches with different K^+ concentrations on both sides of the membrane and 0.5 mM EDTA in the pipette solution. (E) Conductance as a function of concentration for WT and E92A/ D97V/ E104S/ E132Q in the presence and absence of 0.5 mM EDTA. Lines represent best fits to Eq. 1, with g_{max} = 50 pS ± 1 and K_m = 11.0 ± 1.3 mM (WT); g_{max} = 53 ± 1 pS and K_m = 2.2 ± 0.4 mM (WT + EDTA); g_{max} = 47 ± 1 pS and K_m = 12 ± 1 mM (E92A/ D97V/ E104S/E132Q); and g_{max} = 47 ± 2 pS and K_m = 12 ± 2 mM (E92A/ D97V/ E104S/E132Q + EDTA).

(Lu and MacKinnon, 1994a). These results contrast with the concentration dependence seen in other K^+ channel types. Maxi-K channels have apparent K_m values of 50–140 mM (Latorre and Miller, 1983). For Shaker channels, the value is even higher, around 300 mM (Heginbotham and MacKinnon, 1993). KcsA channels show a more complex biphasic concentration dependence with a linear increase in conductance at high concentrations of K^+ (Morais-Cabral et al., 2001).

In evaluating the K^+ concentration dependence, we did not substitute other ions for K^+. If fixed negative charges attract K^+ to the outer mouth of the channels (D'Avanzo et al., 2005; Chang et al., 2010), the change in ionic strength would alter the screening of these charges, making the measured K_m values artificially low. On the other hand, if there is a relatively nonspecific binding site for cations in the outer mouth, the presence of other ions that might compete for this site would make the measured K_m values artificially high. We believe, based on our measurements and as discussed below, that the latter artifact is more important, so we used a protocol without ion substitution.

We focused our attention on concentrations between 5 and 200 mM, where the channels behave as a pseudo–single-ion system:

$$K_o + C \longleftrightarrow K \bullet C \longleftrightarrow K_i + C,$$

where C is the channel, and K_o, $K \bullet C$, and K_i refer to the K^+ ions in the outer solution, bound to the channel and in the inner solution, respectively. In such as system, ion movement through the channel saturates with an apparent K_m value of k_d/k_a that reflects the (voltage-dependent) rates of association to (k_a) and dissociation from (k_d) the binding site. Maximal inward currents are determined by the rate of dissociation to the inner solution. Under bi-ionic conditions, the relative permeability will reflect channel occupancies by the two species; these occupancies will be inversely related to K_m. Such a model is clearly an oversimplification, as both physiological and structural measurements indicate that the channels are multi-ion pores. However, as shown recently (Nelson, 2011), permeation through multi-ion pores can under some conditions still be considered a two-step association–dissociation process that follows Michaelis–Menton kinetics.

In any case, the scheme provides some simple approximations. From the single-channel currents of 5 pA at −100 mV, k_d must be at least $3 \times 10^7\ s^{-1}$ at this voltage. If K_m = 10 mM, the value of k_a would be $>3 \times 10^9\ M^{-1} \bullet s^{-1}$. This is close to the maximum rate of ion capture by diffusion for a pore with an outer mouth of ∼10-Å radius (Hille, 2001). Cation capture rates by the channel may be accelerated by electrostatic attraction to fixed negative charges in the channel mouth.

Rb^+ and NH_4^+ currents

The apparent K_m value for Rb^+ conduction was 24 mM, significantly larger than that for K^+. Rb^+ also has a lower maximal conductance than does K^+ (Fig. 2), and the permeability ratio P_{Rb}/P_K based on bi-ionic reversal potentials is 0.4–0.6 (Chepilko et al., 1995; Choe et al., 2000). This indicates that channel occupancy by K^+ is favored over Rb^+. As channel occupancy would in turn be inversely related to K_m, as discussed above, the higher K_m for Rb^+ is in agreement with the lower permeability. The lower maximal currents indicate a lower rate of dissociation from the channel.

NH_4^+ is a more complicated case. It has a maximal inward conductance similar to that of K^+, but the permeability ratio is ∼0.1 (Chepilko et al., 1995; Choe et al., 2000). This could be explained if permeation barriers for NH_4^+ and K^+ were similar, but that NH_4^+ interacted more weakly than K^+ with binding sites within the channel. Our naive prediction was that the apparent affinity of the pore for NH_4^+ would be lower than that for K^+. Consistent with this notion, the measured K_m value for NH_4^+, 14 mM, is indeed higher than that for K^+. However, the ratio of K_m values ($K_m(NH_4)/K_m(K)$ of <2) is much smaller than that for permeability (P_K/P_{NH4} of ∼10). Outward NH_4^+ currents apparently saturated at lower concentrations. Although these observations are difficult to explain with a simple permeation model, they can be accommodated by a more realistic

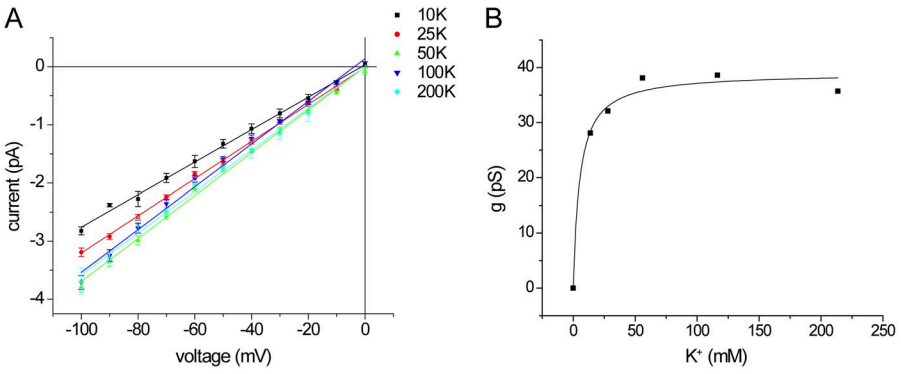

Figure 9. Fixed charges in the transmembrane cavity increase affinity for K^+ permeation. (A) i-V relationships for Kir1.1b N152D in inside-out patches with different symmetrical [K^+]. (B) Conductance as a function of concentration for N152D. Lines represent the best fits to Eq. 1, with g_{max} = 39 ± 2 pS and K_m = 4.7 ± 1.4 mM.

(and more complex) formalism, as shown in Fig. 10 and discussed below.

Outer binding site for cations

The outer mouth of the pore represents one possible location of saturable cation binding. Occupancy of a site in this part of the channel could be rate limiting for conduction, particularly for inward currents. To explore this possibility, we first examined the abilities of impermeant ions to block the channel from the outside. Small divalent cations (Mg^{2+}, Ca^{2+}) blocked Kir1.1 channels with a small but significant voltage dependence ($z\delta$ of ~0.2), consistent with a blocking site within the transmembrane electric field. The affinity of these divalents for the blocking site, assessed as apparent K_i value at constant voltage, was higher for Mg^{2+} than for Ca^{2+}. A similar block of Kir2.1 channels was reported previously (Murata et al., 2002). The impermeant monovalent cations Na^+ and Li^+ also blocked the channels with lower apparent affinity but with a voltage dependence similar to that of Mg^{2+} or Ca^{2+}. Although this could indicate that the monovalent ions penetrate deeper into the electric field, it is also consistent with the idea that monovalents and divalents block at the same site, with the voltage dependence attributable mainly to the movement of K^+ ions within the field consequent to block. Such a scenario was suggested for external TEA^+ interactions of *Shaker* K^+ channels (Thompson and Begenisich, 2003).

Competition between monovalents and divalents indicates that these ions occupy the same outer site, or at least that their binding is mutually exclusive. Based on the ability to relieve Mg^{2+} block, the monovalent cation selectivity for this site is $K^+ > Na^+ \sim Li^+ > Rb^+ \sim NH_4^+$. In particular, the estimated K_d for K^+ displacement of Mg^{2+} was 14 mM, a value not too different from the apparent K_m for conduction. In addition, 3 mM Mg^{2+} added to the outer solution increased the apparent K_m for K^+ conductance substantially. These findings are consistent with the idea that saturation of K^+ conductance involves interaction with this outer binding site. The ability of the other permeant ions, Rb^+ and NH_4^+, to displace Mg^{2+} was less than that of K^+, in qualitative agreement with their lower permeabilities and higher K_m.

The S0 site, lying just outside the selectivity filter of K^+ channels, is a likely structural locus for this outer binding site. This site has been identified in crystal structures of KcsA channels (Zhou et al., 2001) as well as through

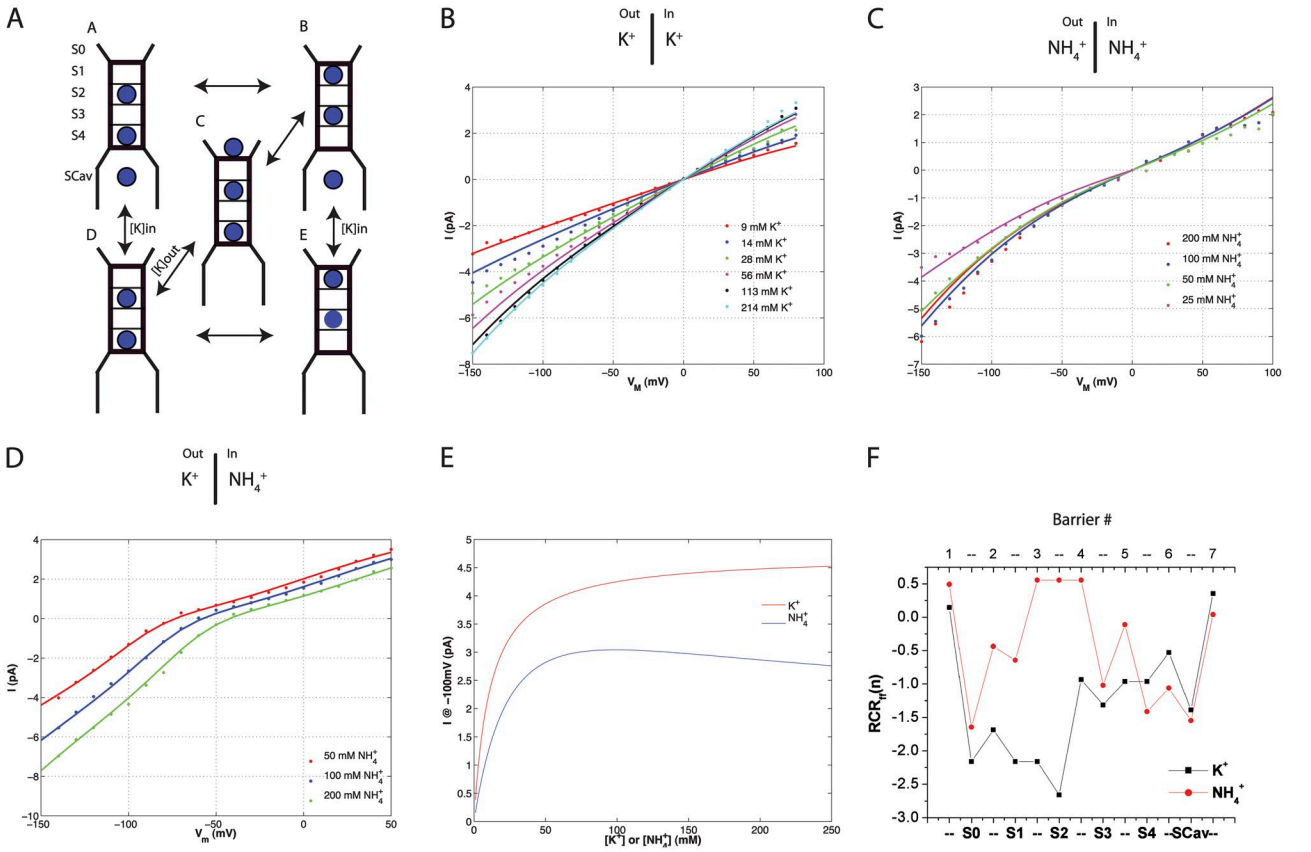

Figure 10. Kinetic model for permeation through Kir1.1 channels. (A) Kinetic scheme with six ion-binding sites and five states. (B) Fits of i-V relationships with symmetrical $[K^+]$. (C) Fits of i-V relationships with symmetrical $[NH_4^+]$. (D) Fits of i-V relationships with fixed internal $[K^+]$ and variable external $[NH_4^+]$. (E) Saturation of K^+ and NH_4^+ currents in the simulated channel. (F) Energy profile for K^+ and NH_4^+ movement through the pore of Kir1.1. The major differences are in the well depths of S1 and S2.

computational modeling (Bernèche and Roux, 2001). Ions associated with the channel at this location are probably partially dehydrated (Bernèche and Roux, 2001). Occupancy and dehydration may be stabilized by electrostatic interactions with negatively charged amino acid side chains (Zhou et al., 2001). If this identification is correct, this site exhibits a significant though modest selectivity for K^+ over Na^+. Another site, termed S_{ext}, was also identified as a locus of ion accumulation in KcsA channels external to S0 (Bernèche and Roux, 2001; Zhou et al., 2001). Blocking at this site is less likely to show an appreciable voltage dependence. The blockers are unlikely to bind deeper within the pore, as this would predict a stronger voltage dependence, at least for divalent cations. If the S1 site senses 25% of the electric field, block at that site by external Mg^{2+} would have a $z\delta$ value of at least 0.5, and probably more because K^+ would be displaced toward the cytoplasm during occupancy of the site by a blocker. The measured was ~0.2. On the other hand, the binding of permeant cations to the S1 site selectivity filter could contribute to the ability of monovalent cations to inhibit Mg^{2+} block at S0, especially in the case of K^+.

The apparent K_m for inward currents was weakly voltage dependent, at least for K^+ and NH_4^+, with a higher K_m estimated when the membrane was hyperpolarized. This could arise if the forward rate of exit from the outer binding site had a higher voltage dependence than the rate of entry onto the site.

We mutated anionic amino acids in the outer mouth that might increase Mg^{2+} and/or K^+ affinities for the channel through favorable electrostatic interactions. As reported previously (Sackin et al., 2011), the elimination of four of these charges (or 16 negative charges per tetramer) still resulted in a functional channel with conductance and kinetics similar to those of the wild-type channel. Mutation of the negatively charged side chain closest to the site, E104S, did indeed decrease the affinity of the channel for Mg^{2+} block; the apparent $K_i(0)$ increased from 4 to 20 mM. The elimination of a negative charge at an adjacent residue in Kir2.1 had a similar effect on Mg^{2+} affinity in Kir2.1 channels (Murata et al., 2002). The removal of the other three negative charges did not further decrease Mg^{2+} affinity of the Kir1.1. The apparent K_m for K^+ conductance did not change significantly either with the single E104S mutation or the quadruple mutation. In part, this reflects the lower valence of K^+, relative to Mg^{2+}, making binding less sensitive to the electrostatic potential. In addition, however, elimination of the screening of the negative charges by trace divalent cations by chelation with EDTA revealed their impact on K_m.

Inner cation-binding site

We also examined the effects of adding negative charges just inside the selectivity filter within the transmembrane cavity. This N152D mutation mimics the natural anionic side chain in Kir2.1 that contributes to the strong block of this channel by intracellular Mg^{2+} and polyamines (Lu and MacKinnon, 1994b; Taglialatela et al., 1995; Yang et al., 1995). The apparent K_m for conductance through this mutant was about half that of the wild-type channel. Thus, this site can also contribute to the saturation behavior of inward rectifiers.

A kinetic model

Our simulations addressed the question of whether standard models of permeation through K^+ channels with designated ion-binding sites identified by x-ray crystallography could explain the observed behaviors. We could identify a set of kinetic parameters that accounted for many of the channel properties, including the low K_m values for both K^+ and NH_4^+, the high K^+/NH_4^+ permeability ratio despite similar maximal conductances, and the increase in inward NH_4^+ conductance with K^+ on the opposite side of the membrane. The model is based on discrete-state kinetics and contains a minimal number of sites consistent with structural information. We do not claim that it is unique in describing the experimental results. However, we believe that the simulations show that our data can be explained without postulating any new or unusual features of the channel or a qualitatively different interaction of NH_4^+ and K^+ ions with the channel.

Analysis of this model helps to explain a major conclusion from experimental findings: two observable parameters related to the strength of interaction of permeant ions with the pore—bi-ionic permeability and apparent affinity—can be dissociated. The relative permeability of ions depends on the energy of binding to all the sites within the multi-ion pore. Saturation of inward conduction through the channels reflects the occupancy of a cation-binding site outside the selectivity filter and is not necessarily correlated with permeability. The similar K_m values for permeant cations reflect the relatively nonspecific cation binding to this part of the channel.

We thank Olaf S. Andersen for helpful comments on the manuscript.

This work was supported by grants RO1-DK27847 (to L.G. Palmer) and RO1- DK46950 (to H. Sackin) from the National Institutes of Health.

Ted Begenisich served as guest editor.

Submitted: 3 October 2011
Accepted: 13 January 2012

REFERENCES

Andersen, O.S. 1999. Graphic representation of the results of kinetic analyses. *J. Gen. Physiol.* 114:589–590. http://dx.doi.org/10.1085/jgp.114.4.589

Bernèche, S., and B. Roux. 2001. Energetics of ion conduction through the K+ channel. *Nature.* 414:73–77. http://dx.doi.org/10.1038/35102067

Chang, H.K., J.R. Lee, T.A. Liu, C.S. Suen, J. Arreola, and R.C. Shieh. 2010. The extracellular K+ concentration dependence of outward currents through Kir2.1 channels is regulated by extracellular Na+ and Ca2+. *J. Biol. Chem.* 285:23115–23125. http://dx.doi.org/10.1074/jbc.M110.121186

Chepilko, S., H. Zhou, H. Sackin, and L.G. Palmer. 1995. Permeation and gating properties of a cloned renal K^+ channel. *Am. J. Physiol.* 268:C389–C401.

Choe, H., H.S. Sackin, and L.G. Palmer. 2000. Permeation properties of inward-rectifier potassium channels and their molecular determinants. *J. Gen. Physiol.* 115:391–404. http://dx.doi.org/10.1085/jgp.115.4.391

D'Avanzo, N., H.C. Cho, I. Tolokh, R. Pekhletski, I. Tolokh, C. Gray, S. Goldman, and P.H. Backx. 2005. Conduction through the inward rectifier potassium channel, Kir2.1, is increased by negatively charged extracellular residues. *J. Gen. Physiol.* 125:493–503. http://dx.doi.org/10.1085/jgp.200409175

Edvinsson, J.M., A.J. Shah, and L.G. Palmer. 2011. Kir4.1 K+ channels are regulated by external cations. *Channels (Austin).* 5:269–279. http://dx.doi.org/10.4161/chan.5.3.15827

Heginbotham, L., and R. MacKinnon. 1993. Conduction properties of the cloned *Shaker* K^+ channel. *Biophys. J.* 65:2089–2096. http://dx.doi.org/10.1016/S0006-3495(93)81244-X

Hille, B. 2001. Ionic Channels of Excitable membranes. Third Edition. Sinauer Associates, Sunderland, MA. 814 pp.

Kutluay, E., B. Roux, and L. Heginbotham. 2005. Rapid intracellular TEA block of the KcsA potassium channel. *Biophys. J.* 88:1018–1029. http://dx.doi.org/10.1529/biophysj.104.052043

Latorre, R., and C. Miller. 1983. Conduction and selectivity in potassium channels. *J. Membr. Biol.* 71:11–30. http://dx.doi.org/10.1007/BF01870671

Lopatin, A.N., and C.G. Nichols. 1996. [K+] dependence of open-channel conductance in cloned inward rectifier potassium channels (IRK1, Kir2.1). *Biophys. J.* 71:682–694. http://dx.doi.org/10.1016/S0006-3495(96)79268-8

Lu, Z., and R. MacKinnon. 1994a. A conductance maximum observed in an inward-rectifier potassium channel. *J. Gen. Physiol.* 104:477–486. http://dx.doi.org/10.1085/jgp.104.3.477

Lu, Z., and R. MacKinnon. 1994b. Electrostatic tuning of Mg^{2+} affinity in an inward-rectifier K^+ channel. *Nature.* 371:243–246. http://dx.doi.org/10.1038/371243a0

Morais-Cabral, J.H., Y. Zhou, and R. MacKinnon. 2001. Energetic optimization of ion conduction rate by the K^+ selectivity filter. *Nature.* 414:37–42. http://dx.doi.org/10.1038/35102000

Murata, Y., Y. Fujiwara, and Y. Kubo. 2002. Identification of a site involved in the block by extracellular Mg^{2+} and Ba^{2+} as well as permeation of K^+ in the Kir2.1 K^+ channel. *J. Physiol.* 544:665–677. http://dx.doi.org/10.1113/jphysiol.2002.030650

Nelson, P.H. 2011. A permeation theory for single-file ion channels: one- and two-step models. *J. Chem. Phys.* 134:165102. http://dx.doi.org/10.1063/1.3580562

Sackin, H., M. Nanazashvili, H. Li, L.G. Palmer, and L. Yang. 2011. Modulation of kir1.1 inactivation by extracellular Ca and Mg. *Biophys. J.* 100:1207–1215. http://dx.doi.org/10.1016/j.bpj.2011.01.032

Taglialatela, M., E. Ficker, B.A. Wible, and A.M. Brown. 1995. C-terminus determinants for Mg^{2+} and polyamine block of the inward rectifier K^+ channel IRK1. *EMBO J.* 14:5532–5541.

Thompson, J., and T. Begenisich. 2003. External TEA block of shaker K^+ channels is coupled to the movement of K^+ ions within the selectivity filter. *J. Gen. Physiol.* 122:239–246. http://dx.doi.org/10.1085/jgp.200308848

Yang, J., Y.N. Jan, and L.Y. Jan. 1995. Control of rectification and permeation by residues in two distinct domains in an inward rectifier K^+ channel. *Neuron.* 14:1047–1054. http://dx.doi.org/10.1016/0896-6273(95)90343-7

Zhou, Y., J.H. Morais-Cabral, A. Kaufman, and R. MacKinnon. 2001. Chemistry of ion coordination and hydration revealed by a K^+ channel-Fab complex at 2.0 A resolution. *Nature.* 414:43–48. http://dx.doi.org/10.1038/35102009